

# Immelman turn

## A flight mechanics study

Irene Simó Muñoz  
irene.munoz@estudiantat.upc.edu

Prof: Àlex Ferrer Farré  
Fall 2021

This brief project aims to take a look at the flight mechanics involved in the Immelmann turn maneuver while analysing its performance in a realistic context.

For this, a first set of computations have been performed in order to obtain the models of the physic phenomena occurring, and a later sutdy with aircraft values has been carried out to evaluate the previously obtained results.

All the coding has been done with MATLAB<sup>1</sup> version R2021b (September 2021). The git repository of this project, including the LATEXfiles, can be found in [this link](#).

This project has been developed for course 22027-Mecànica del vol in the Grau en Enginyeria en Tecnologies Aeroespacials degree, Universitat Politècnica de Catalunya, during fall 2021.

## Contents

Introduction . . . . .	1
Maneuver Computations . . . . .	1
First phases - cruise . . . . .	2
Second phase - semicircle . . . . .	2
Third phase - inversion . . . . .	2
Forth phase - cruise . . . . .	2
Maneuver study . . . . .	2
Cruise flight . . . . .	3
Half loop . . . . .	4
Roll . . . . .	6
Trajectory analysis . . . . .	7
Bibliography	9
List of Figures	9

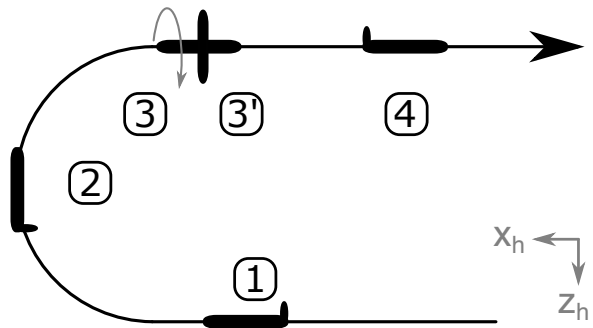


**Figure 1** Immelman turn overview. Own elaboration.

The aircraft initiates this maneuver in straight levelled flight, and describes an upwards semicircle contained in its symmetry plane. This increases the flight altitude while changing the trajectory's to the original's opposite direction and leaves the plane turned upside down. It then rolls while still flying in a straigth line, and returns to the initial condition of levelled flight.

This maneuver can be performed for various velocities and radius, but there are some dependencies and limitiations to be taken into account, such as the maximum deflections or forces the control surfaces can provide or support, respectively.

In order to cover all these variables, a first approach through the dynamic and kinetic equations follows.

## Introduction

The Immelman turn, named after German World War I flying ace Max Immelmann, is an an aerobatic maneuver that results in level-flight of the aircraft in the opposite direction and higher altitude.

## Maneuver Computations

Let us assume symmetric flight (no lateral aerodynamic force  $Q = 0$  nor lateral thrust force as  $\nu = 0$ ), the thrust generated by the engines is parallel to the  $x$  wind axis (thus  $\epsilon = 0$ ), and that the maneuver takes place flawlessly, this is in the vertical plane too;  $\xi = \dot{\xi} = 0$ .

<sup>1</sup>MATrix LABoratory, language developed by The MathWorks Inc.

As the maneuver is a rather short, we will also assume that the fuel consumed is negligible and no mass fraction is lost;  $\dot{m} = 0$ .

The motion equations follow [3]:

$$\left\{ \begin{array}{l} T \cos(\epsilon) \cos(\nu) - D - mg \sin \gamma - m \dot{V} = 0 \\ T \cos(\epsilon) \sin(\nu) - Q + mg \cos \gamma \sin \mu + \dots \\ \dots + mV(\dot{\gamma} \sin \mu - \dot{\Xi} \cos \gamma \cos \mu) = 0 \\ -T \sin \epsilon - L + mg \cos \gamma \cos \mu + \dots \\ \dots + mV(\dot{\gamma} \cos \mu - \dot{\Xi} \cos \gamma \sin \mu) = 0 \\ \dot{x}_e = V \cos \gamma \cos \Xi \\ \dot{y}_e = V \cos \gamma \sin \Xi \\ \dot{z}_e = -V \sin \gamma \end{array} \right.$$

And for each of the phases that compose the maneuver, they can be simplified by substituting the flight conditions.

	$\mu$	$\gamma = \dot{\gamma}$	$\xi = \dot{\xi} = \nu = \epsilon = Q$
Cruise	0	0	0
Semicircle	0	f(t)	0
Inversion	f(t)	0	0

## First phases - cruise

$$\left\{ \begin{array}{l} T - D - m \dot{V} = 0 \\ 0 = 0 \\ -L + mg = 0 \\ \dot{x}_e = V \\ \dot{y}_e = 0 \\ \dot{z}_e = 0 \end{array} \right. \quad (1)$$

There are three equations and four variables;  $\alpha$ ,  $\pi$  and  $V$ . Total degrees of freedom is one, although in further study both  $\alpha$  and  $\pi$  will be fixated.

## Second phase - semicircle

$$\left\{ \begin{array}{l} T - D - mg \sin \gamma - m \dot{V} = 0 \\ 0 = 0 \\ -L + mg \cos \gamma + mV \dot{\gamma} = 0 \\ \dot{x}_e = V \cos \gamma \\ \dot{y}_e = 0 \\ \dot{z}_e = -V \sin \gamma \end{array} \right. \quad (2)$$

There are four equations and four variables:  $\alpha$ ,  $\pi$ ,  $V$  and  $\gamma$ . The elevator and gas control lever or throttle are for controlling  $\alpha$  and  $\pi$  respectively. In further study both of them will be fixed.

## Third phase - inversion

$$\left\{ \begin{array}{l} T - D - m \dot{V} = 0 \\ mg \sin \mu = 0 \\ -L - mg \cos \mu = 0 \\ \dot{x}_e = V \\ \dot{y}_e = 0 \\ \dot{z}_e = 0 \end{array} \right. \quad (3)$$

There are three equations and five variables;  $\alpha$ ,  $\pi$ ,  $V$  and  $\mu$ . Except from the velocity, they can be controlled by the pilot through the elevator deflection, gas lever and ailerons respectively. Total degrees of freedom are, therefore, 2. In further study both the elevator deflection and gas lever will be fixated.

## Forth phase - cruise

$$\left\{ \begin{array}{l} T - D - m \dot{V} = 0 \\ 0 = 0 \\ -L + mg = 0 \\ \dot{x}_e = V \\ \dot{y}_e = 0 \\ \dot{z}_e = 0 \end{array} \right. \quad (4)$$

There are three equations and four variables;  $\alpha$ ,  $\pi$  and  $V$ . The dynamics are identical to those in the first phase, as both of them are cruise flight.

## Maneuver study

The higher the velocity is, the bigger the radius - this is, the greater the increase of altitude - given that the wing's flaps cannot deflect enough nor can support as much force to reduce the radius as to the same maneuver for a lower velocity.

Note that the centripetal force follows:

$$F = \frac{mV^2}{R}$$

Where  $m$ ,  $V$  and  $R$  are the aircraft's mass (in kg), velocity (in m/s) and radius (in m) respectively.

The only angles affected are gamma  $\gamma$  and mu  $\mu$  if performed flawlessly. The former is the angle formed between the  $x$  axis of the horizontal set and the  $x$  axis of the wind set, while the latter is the one formed between the  $y$  axis of the same sets. Note that for the whole maneuver the body set remains consistent with the wind set.

Figure 2 shows how these change in the different phases of the Immelmann turn

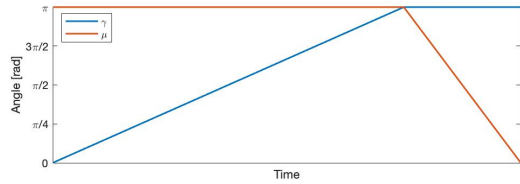


**Figure 2** Angles evolution over time

Note that for  $\gamma$  the evolution is perfectly defined, as the increment of said angle needs to be positive in order to increase the flight altitude. Conversely, for  $\mu$  the pilot could choose to rotate in the opposite direction thus changing  $\mu$  from 0 to  $-\pi$  instead - note that  $\pi$  and  $-\pi$  are equivalent -, and the result would be virtually the same.

Furthermore, in order to describe a perfect semicircle the angular speed  $\dot{\gamma}$  needs to remain constant. This results in the necessary condition of gamma's evolution to be a straight slope. For  $\mu$ , however, the pilot could also perform the roll at non-constant rotating speed without this having an impact on the maneuver performance. This would be reflected as a curve on mu's temporal evolution, instead of a straight line.

All these For the following computations, some values will be needed in order to numerically solve the Ordinal Differential Equation systems. The ENAERT T-35 Pillán, a Chilean military small aircraft and its data [2] have been taken as references.



**Figure 3** ENAERT T-35 Pillán. Extracted from [1]

The used information is:

	Value		Value
Mass	1.300 kg	Wingspan	8.84 m
Airfoil	63 <sub>3</sub> -414	Wing area	13.69 m <sup>2</sup>
Stall s.	31.94 m/s	Cruise s.	70.84 m/s
Thrust	224 kW	Air den.	1.225 kg/m <sup>3</sup>
$C_L = 12\alpha + 0.33$			

The selected initial speed is of 70 m/s as the third phase of the maneuver requires a few less meters per second in order to be performed safely.

For the totality of the maneuver, the fixated parameters are the gas control lever ( $\pi$ ) and the elevator ( $\alpha$ ), which are set as constants at 1.5 kN and 0.3 rad respectively. From the remaining variables, the position coordinates evolution ( $x$  and  $z$ ) are always left as dependant in order to be solved by the ODE solver. With the obtained results, the trajectory is plot - see the following section Trajectory analysis, where both of them are studied in moer depth -.

$$L = \frac{1}{2} S \rho V(t)^2 C_L(\alpha) \quad (5)$$

$$D = \frac{1}{2} S \rho V(t)^2 C_D(\alpha) \quad (6)$$

### Cruise flight

For the first and last phases, both cruise flight, the remaining variable (not counting  $\dot{x}$  and  $\dot{z}$ ) is velocity ( $V$ ) alone.

As fixed thrust and elevator deflection are imposed, there are virtually no temporal changes affecting velocity. This results in constant speed or cruise flight, and a simple slope regarding the x-axis position. When computing both the lift and drag forces, these must be constant too - see equations 5 and 6 -.

Velocity being constant results in both lift and drag being constant too.

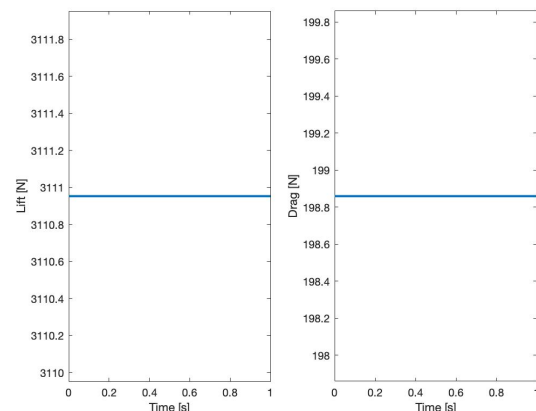


**Figure 4** Radius dependance on  $V$  and  $\alpha$ t. Own elaboration.

In regards of the general overview, cruise flight is quite straight forward, as both the speed and vertical position remain constant, and as velocity is linealry dependant on time, the displacement of the aircraft is linear as well.

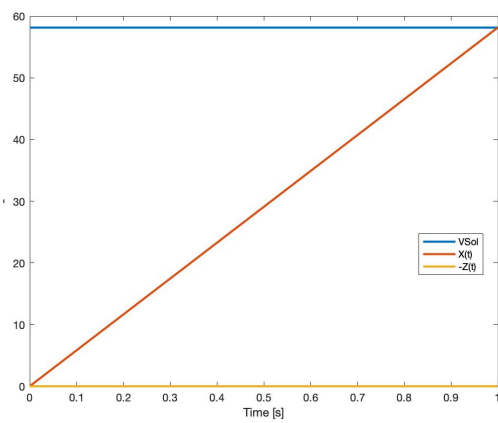


**Figure 5** Radius dependence on  $V$  and  $\alpha_t$ . Own elaboration.

For the total time, the following integration from the first equation can be done:

$$dt = \frac{m}{T - D} dV$$

$$\int dt = \int \frac{m}{T - D} dV$$

Substituting drag's definition from equation 6 and operating for lineal aerodynamics,

$$= \int_{V_0}^V \frac{m}{T - \frac{1}{2}\rho SV^2(C_{D_0} + kC_L^2)} dV$$

$$t_1 = \frac{m}{T - \frac{1}{2}\rho SV^2(C_{D_0} + kC_L^2)} (V - V_0)$$

## Half loop

In order to work with the half loop part of the maneuver, some preliminary of the trajectory geometry is done. The three force configurations during the maneuver correspond to the free body diagrams at stages 1, 2 and 3 (see Figure 1).

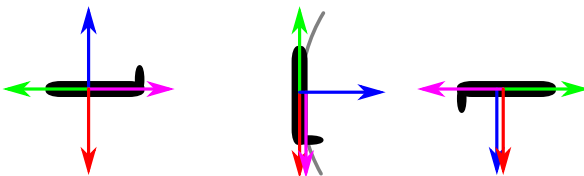


**Figure 6** Free body diagrams during the semiloop. Own elaboration.

Note that at all times the lift behaves as the centripetal force, thus indicating that both the velocity and radius limitations to perform the Immelmann turn are inherent to the wing design and its maximum and minimum lift generation.

As the motion will be circular, the normal and tangential accelerations will follow:

$$a_n = \frac{V^2}{R} = V\dot{\gamma} = \dot{\gamma}^2 R \quad a_t = V^2 R$$

As a result, the radius can be written as a function of the angle of attack. By operating with the third equation of system number 2, which is in wind system of reference, very convenient as is also polar set of axis:

$$L = m \left( \frac{V^2}{R} + g \cos(\gamma) \right)$$

$$\frac{1}{2} \rho SV^2 C_L(\alpha) = m \left( \frac{V^2}{R} + g \cos(\gamma) \right)$$

$$R = \frac{2mV^2}{2W \cos(\gamma) + \rho SV^2 C_L(\alpha)}$$

As the plane must describe a semicircle, the radius must be constant.

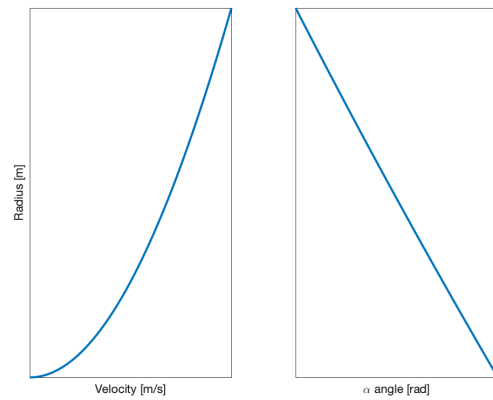


**Figure 7** Radius dependence on  $V$  and  $\alpha_t$ . Own elaboration.

For this phase the evolution of  $\gamma$  will be imposed. By using the following conditions:

- Must begin at 0 and end at  $\pi$  rad
- Must have a linear evolution throughout time - in order not to overcomplicate the problem -
- Must be compatible with circular accelerations, as the ideal performance of the maneuver would require the half loop to be a semicircle

From these it can clearly be deduced that the basic model for a slope will be required

$$\gamma(t) = At + B$$

And the rest of conditions define the parameters A and B such that the resulting expression is obtained:

$$\gamma(t) = \frac{V_0}{R} t \quad \text{or} \quad \gamma(t) = \frac{V_0}{R} t + \pi - \frac{V_0}{R} t_f \quad (7)$$

Where the finishing time of  $t_f$  would be  $t_f = \pi/V_0$ . Note that  $V_0$  instead of  $V(t)$  has been employed. This is in order to ensure the linearity, although a time dependant velocity could be used too. This would lead to a concatenation of curves for the loop, and not a semicircle.

Given that the determined parameters are therefore the gas control lever ( $\pi$ ) and the elevator ( $\alpha$ ), with the same values as for the previous phase - 1.5 kN and 0.3 rad respectively -, but also  $\gamma$  is, the only variable to study is the velocity. Note that the position coordinates evolution ( $\dot{x}$  and  $\dot{z}$ ) are explored in the following section: Trajectory analysis.

For this phase, the velocity must follow a non-linear evolution as it is dependant on both trigonometric and squared terms in the equations, see  $\gamma$  and the lift and drag forces definitions in equations 5 and 6. As the previous schemes in Figure 6 show, at the vertical flight after a quarter of loop, the velocity slows its rate of increase at that point. This inflection point is the consequence of the weight force switching the aircraft's axis for  $\gamma = \pi/2$  thus forcing a force redistribution in order to maintain equilibrium.

As Figure 8 shows, it is worth noting too that the higher the initial speed solely modifies the placement of the curve in the plot, but has no effect on its characteristics. Although it is not clearly shown in the plot, the time is reduced too. On the contrary, for a fixed velocity, different radii have a more noticeable impact on the performance of the semiloop. As greater radius require more time to get to the quarter loop point - for the same initial speed -, the local velocity maximum prior to the  $\gamma = \pi/2$  state is higher the greater the radius. Although both the local maximum and the finishing speed are higher, the greater the radius the longer it takes to complete the half loop.

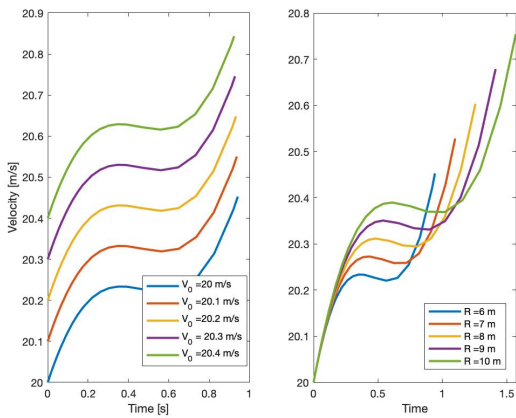


**Figure 8** Radii and velocity dependencies on the half loop. Own elaboration.

Both the lift and drag are affected by this velocity oscillation, but its magnitude is rather small when compared to the rest of the parameters'.

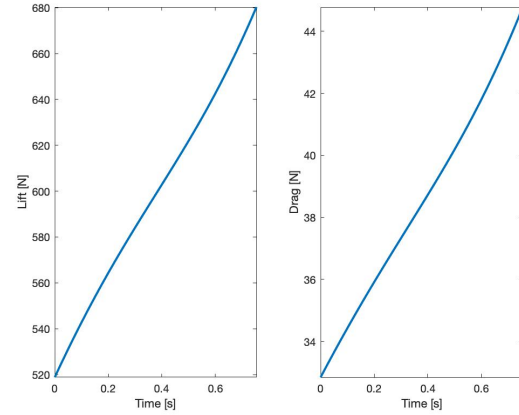


**Figure 9** Lift and drag on the half loop. Own elaboration.

Lastly, both of the position coordinates evolution ( $\dot{x}$  and  $\dot{z}$ ) evolve as expected, this is, highly dependant on  $\gamma$ . As this angle ranges from 0 to  $\pi$ , both coordinates follow reasonable behaviours. It is also clearly shown that the speed remains fairly constant during this part of the maneuver too.

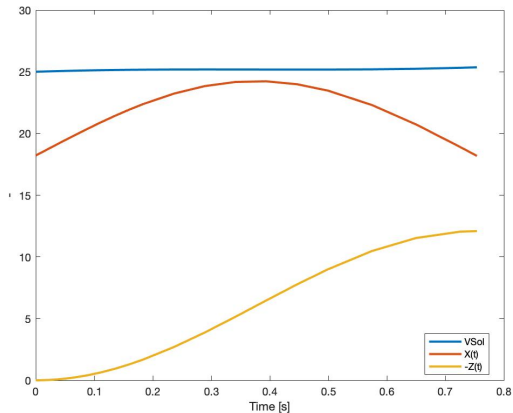


**Figure 10** Radii and velocity dependencies on the half loop. Own elaboration.

For time integration in this case

$$\begin{cases} \frac{\partial V}{\partial t} = \frac{1}{m} (T - D - mg \sin \gamma) \\ \frac{\partial \gamma}{\partial t} = \frac{1}{mV} (L - mg \cos \gamma) \end{cases}$$

As during this phase the angle  $\gamma$  must evolve from 0 to  $\pi$  rad -for simplification purposes we will work

with a linear model - and, as previously stated, the circular motion accelerations have been assumed to apply, we can write:

$$\gamma(t) = \frac{V}{R} t \quad \frac{\partial \gamma(t)}{\partial t} = \frac{V}{R}$$

$$dt = \frac{m}{T - D - mg \sin \gamma} dV$$

$$\int dt = \int \frac{m}{T - D - mg \sin \gamma} dV$$

Substituting drag's definition from equation 6 and operating for lineal aerodynamics,

$$= \int \frac{m}{T - \frac{1}{2} \rho S V^2 (C_{D_0} + k C_L^2) - mg \sin \gamma} dV$$

Substituting ,

## Roll

Similarly to the half loop, for this phase a part of the known fixed parameters; gas control lever ( $\pi$ ) and elevator deflection ( $\alpha$ ) more conditioning is needed. In this case, the angle is the roll angle;  $\mu$ . As previously done for  $\gamma$ , the conditions for  $\mu$  are:

- Must begin at  $\pi$  (or  $-\pi$ ) and end at 0 rad
- Must have a linear evolution throughout time - in order not to overcomplicate the problem -

From these it can clearly be deduced that the basic model for a slope will be required

$$\mu(t) = At + B$$

As we are missing some conditions to determine the rate at which the aircraft should roll, the selection is based on the aircraft's structural capacities. For aerobatic aircrafts the rolls must be performed at approximately 120 knots for full aileron rolls and a rotating velocity of 7 m/s at the tip of the wing. With this data and the wingspan we can extract the expressions:

$$\mu(t) = -\frac{V_{tip}}{b/2} t + \pi \quad (8)$$

or

$$\mu(t) = -\frac{V_{tip}}{b/2} t + \pi - \frac{V_{tip}}{b/2} t_f \quad (9)$$

Where the finishing time of  $t_f$  would be  $t_f = \pi \frac{b/2}{V_{tip}}$ . If the evolution of  $\mu$  is considered, though, it can be seen that between  $\pi$  and  $\pi/2$  its trigonometric value for cosine is negative. For the equation that yields the velocity - squared velocity - this is rather problematic.

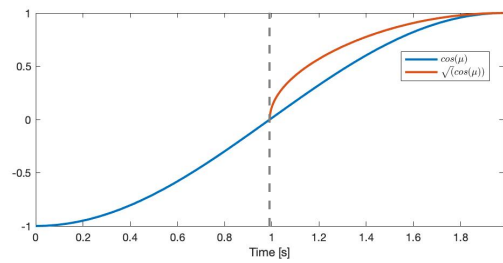


**Figure 11** Unsolvable domain of part of the trajectory. Own elaboration.

For this reason, the computations have been done only for half of the phase, understanding that the remaining quarter of roll is symmetric.

The velocity is deeply conditioned by the values that  $\mu$  acquires throughout the roll, even tending to infinity due to the previously mentioned trigonometric properties. In reality, we can assume a small variation of the total lift and drag, which would be oscillating between the lower values of the plots from Figure 12.

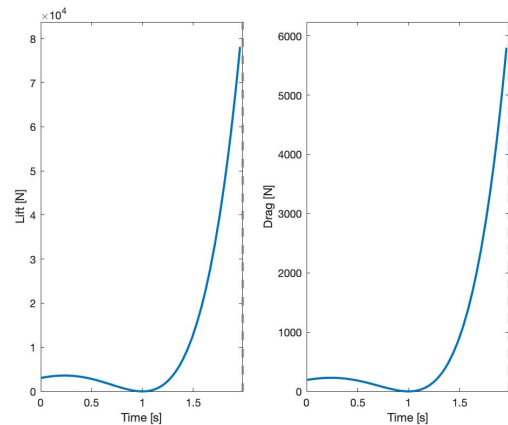


**Figure 12** Unsolvable domain of part of the trajectory. Own elaboration.

For the general overview:

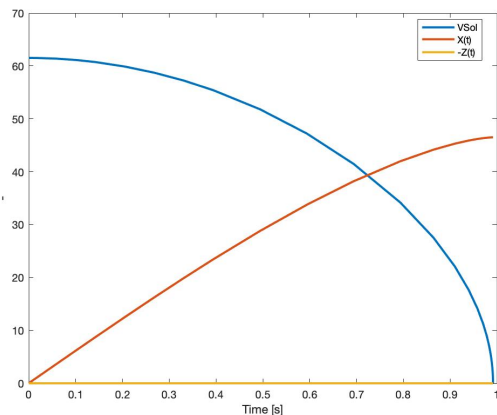


**Figure 13** Radii and velocity dependencies on the half loop. Own elaboration.

The total velocity and  $x(t)$  would continue symmetrically; the velocity would rapidly increase again and the position would exit the inflection point to keep increasing again.

Temporal integration is exactly equal to the cruise phase one, as the roll does not have an effect on the temporal derivatives.

$$dt = \frac{m}{T - D} dV$$

$$\int dt = \int \frac{m}{T - D} dV$$

Substituting drag's definition from equation 6 and operating for lineal aerodynamics,

$$t_1 = \int_{V_0}^V \frac{m}{T - \frac{1}{2}\rho SV^2(C_{D0} + kC_L^2)} dV$$

$$t_1 = \frac{m}{T - \frac{1}{2}\rho SV^2(C_{D0} + kC_L^2)} (V - V_0)$$

Note that this phase of the maneuver is perhaps the most idealised, as a roll is an unbalanced maneuver. Because of the aircraft stability design adverse yaw appears from the very beginning. In a nutshell, an aircraft performing an aileron roll will actually fly along a slightly helical path, and a very light, positive g force will be maintained.

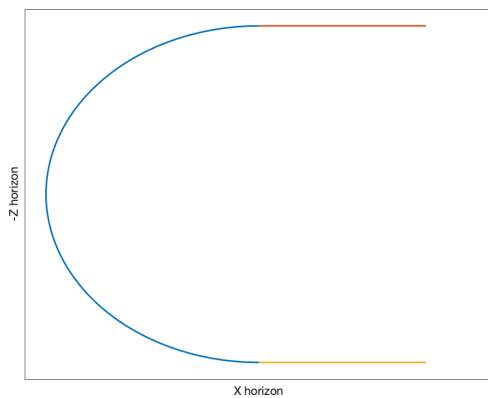
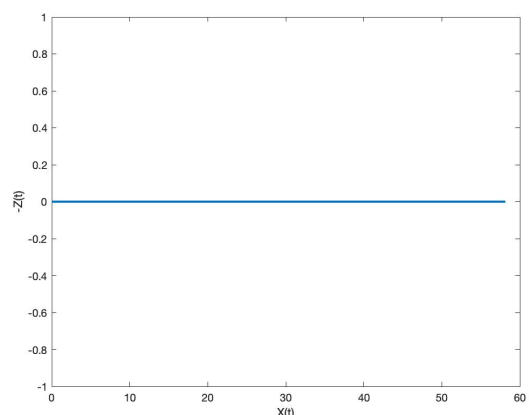


**Figure 14** Expected trajectory output. Own elaboration.

We can consider the maneuver coordinates:

$$\begin{aligned} \dot{x}_e &= V \cos \gamma & x_e &= Vt \cos \gamma \\ \dot{y}_e &= 0 & y_e &= 0 \\ \dot{z}_e &= -V \sin \gamma & z_e &= -Vt \sin \gamma \end{aligned}$$

From the computational results obtained from ODE solvers, the following plots represent the trajectory:



## Trajectory analysis

The expected result of the trajectory is portrayed in the following image:

**Figure 15** Trajectory output for cruise flight. Own elaboration.

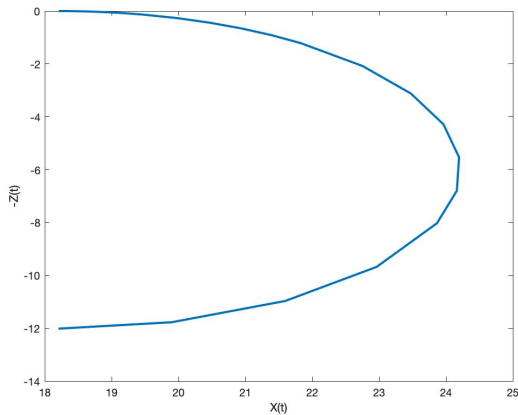


**Figure 16** Trajectory output for the semiloop. Own elaboration.

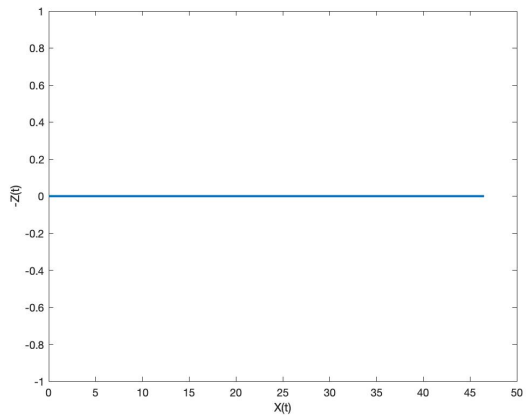


**Figure 17** Trajectory output for the roll. Own elaboration.

The obtained results fit perfectly with the expected output.

# Bibliography

- [1] Cristian Marambio Defensa.com. Proyecto t-35 pillán ii: Nueva vida para el pillán, Apr 2018.
- [2] Frederick Thomas Jane. *Jane's All the World's Aircraft 1913*. David & Charles Reprints, 1969.
- [3] Miguel Ángel Gómez Tierno, Manuel Pérez Cortés, and César Puentes Márquez. *Mecánica del vuelo*. Ibergaceta, 2012.

# List of Figures

1	Immelman turn overview. Own elaboration.	1
2	Angles evolution over time	3
3	ENAERT T-35 Pillán. Extracted from [1]	3
4	Radius dependance on V and $\alpha_t$ . Own elaboration.	3
5	Radius dependance on V and $\alpha_t$ . Own elaboration.	4
6	Free body diagrams during the semiloop. Own elaboration.	4
7	Radius dependance on V and $\alpha_t$ . Own elaboration.	4
8	Radii and velocity dependencies on the half loop. Own elaboration.	5
9	Lift and drag on the half loop. Own elaboration.	5
10	Radii and velocity dependencies on the half loop. Own elaboration.	5
11	Unsolvable domain of part of the trajectory. Own elaboration.	6
12	Unsolvable domain of part of the trajectory. Own elaboration.	6
13	Radii and velocity dependencies on the half loop. Own elaboration.	7
14	Expected trajectory output. Own elaboration.	7
15	Trajectory output for cruise flight. Own elaboration.	7
16	Trajectory output for the semiloop. Own elaboration.	8
17	Trajectory output for the roll. Own elaboration.	8
18	Lift and drag on the cruise phase. Own elaboration.	10
19	Lift and drag on the cruise phase. Own elaboration.	10
20	Lift and drag on the half loop. Own elaboration.	10
21	Lift and drag on the half loop. Own elaboration.	10
22	Lift and drag on the half loop. Own elaboration.	11
23	Lift and drag on the half loop. Own elaboration.	11

## Appendix: Curve fitting

In order to plot the evolution of both Lift and Drag for each phase, the computed velocity - solved from each respective ODE system - has been fitted from the resultant set of data points into a curve. For this, the native `polyfit` and `poly2sym` MATLAB functions have been employed.

To correctly fit a set of points into a curve and avoid overfitting the polynomial (thus dealing with excessive oscillations and Runge's phenomenon among others), the linear Least Squares Method (LLS) has been used. The following plots show the square root sum and the norm of the squared regression value for each phase's velocity fit.

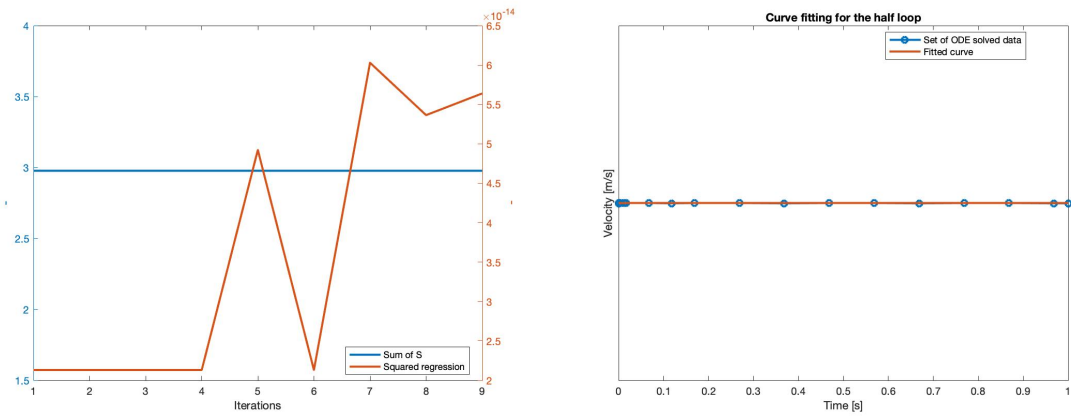


**Figure 18** Lift and drag on the cruise phase. Own elaboration.

**Figure 19** Lift and drag on the cruise phase. Own elaboration.

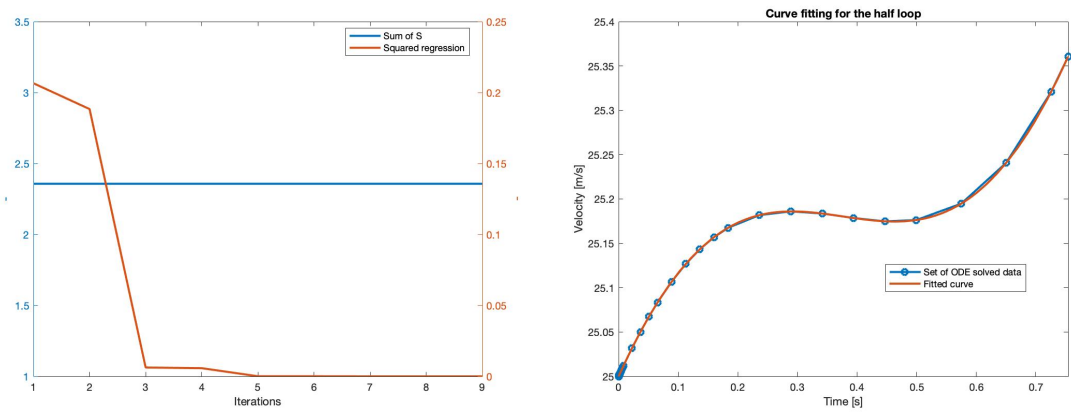


**Figure 20** Lift and drag on the half loop. Own elaboration.

**Figure 21** Lift and drag on the half loop. Own elaboration.

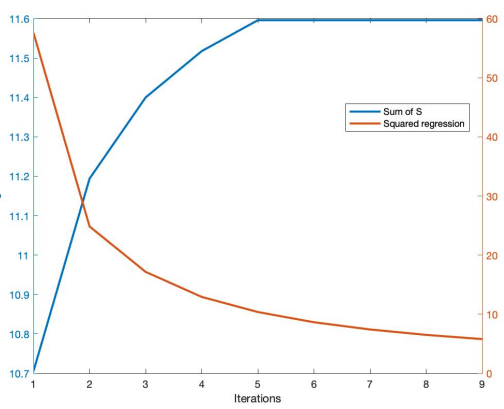


**Figure 22** Lift and drag on the half loop. Own elaboration.

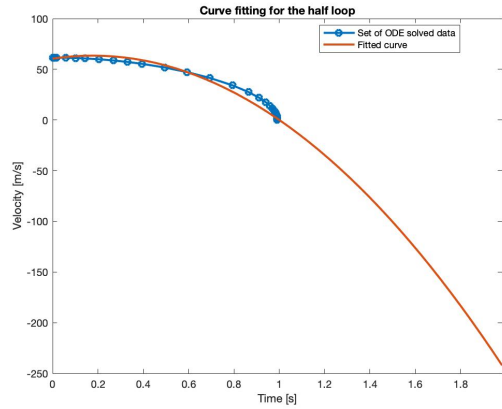


**Figure 23** Lift and drag on the half loop. Own elaboration.